Experimental Investigation of the Linear Viscoelastic Response of EVA-Based Nanocomposites

Ranjit Prasad, Rahul K. Gupta, Ferenc Cser, Sati N. Bhattacharya

Rheology and Materials Processing Centre, School of Civil and Chemical Engineering, RMIT University, Melbourne, Australia

Received 22 March 2005; accepted 1 June 2005
DOI 10.1002/app.22331
Published online 11 May 2006 in Wiley InterScience (www.interscience.wiley.com).

ABSTRACT: Linear viscoelastic behaviors of ethylene-vinyl acetate (EVA)-layered silicate nanocomposites were investigated. EVA with vinyl acetate (VA) content of 18 and 28% by weight and commercially modified montmorillonite clay (Cloisite® 30B) were melt blended in a twin-screw extruder. Nanocomposites of 2.5, 5 and 7.5% by weight were produced. Wide angle X-ray scattering was used to ascertain the degree of layer swelling that could be attributed to the intercalation of polymer chains into the interlayer of the silicates. Transmission electron microscopy was used to analyze the dispersion and extent of exfoliation of the layered silicates in the polymer matrix. All nanocomposites were found to have mixed intercalated/exfoliated morphologies. Both storage and loss moduli and complex viscosity showed improvement at all frequencies tested with increase in silicate loading. Terminal zone behavior was also shown to disappear gradually with silicate content. Increase in silicate loading had caused the divergence of viscosity profile from low-frequency Newtonian plateau to non-Newtonian slope corresponding to a possible finite yield stress. The gradual disappearances of terminal zone and Newtonian homopolymer-like characteristics with silicate loading were attributed to the formation of lattice spanning three-dimensional network structures. J Appl Polym Sci 101: 2127–2135, 2006

Key words: EVA nanocomposites; WAXS; TEM; viscoelastic properties; microstructure

INTRODUCTION

The addition of fillers and reinforcements has played a major role in the plastics industry.[1] Many different types of fillers have been introduced in plastics to provide a synergistic improvement to their properties, for example, tensile strength, heat distortion temperatures, and thermal and electrical conductivities.[1,2] It has also been established that addition of high fractions (weight or volume) of fillers has resulted in considerable changes in rheological properties. Examples of these fillers are small solid particles of carbon black, calcium carbonate, glass fibers, and talc.[1–4] Their particle size range is usually in the micron-level.

Over the last two decades, the addition of nanosized layered silicates in plastics has been found to offer improvements to aforementioned properties, with just a small quantity, typically in the range of 5 wt %. These materials normally called polymer-layered silicates nanocomposites have gained tremendous interest in both the academic and research fields because of their unique structure as well as properties.[5] Layered silicates have been found to be useful in the design of nanocomposites due to their lamellar elements that have high in-plane strength and stiffness and a high aspect ratio (>50). The clay material has a very high surface area of about 750 m^2/g (e.g., montmorillonite).

Structurally, polymer–clay complexes can be classified as phase separated, intercalated, or exfoliated,[6] depending on the nature of components and the preparation technique. Phase separated refers to composites that maintain the immiscibility between the polymer and their inorganic filler. There is minimal reinforcement with respect to this structure. Intercalated structures are obtained when polymer chains have penetrated between the layers of silicates, resulting in expansion of intergallery spacing. Because of mechanical shearing forces and interactions between the silicates and the polymer, the stacks of layered silicates may have dispersed and distributed within the matrix, thus increasing surface area of contact with the polymer. Intercalated structures have been reported to have regions of high and low reinforcements.[7] Exfoliated morphologies result when individual layers (~1 nm) or small stacks of just a few layers are well dispersed and distributed throughout the polymer matrix. The average distance between them depends on the filler concentration. This structure facilitates maximum reinforcement due to huge surface area of contact with the matrix.

Correspondence to: S. N. Bhattacharya (Satinath.Bhattacharya@rmit.edu.au).

TABLE I
Properties of EVA Used in the Project

Properties	EVA18	EVA28
M_w	72,600	58,300
Poly dispersity	8.7	6.2
MFI (g/10 min) (ASTM D 1238)	2.5	25
Peak melting temperature (°C) (ASTM D3417)	88	70
Uses	Film, coextrusion, stretch films	Film packaging

Melt rheological properties are dictated by a combination of mesoscopic structure and the strength of the interaction between the polymer and the layered silicate. Further, the mesoscopic structure would be crucially dependent not only on the strength of the polymer/layered silicate interaction, but also on the inherent viscoelastic properties of the matrix in which the layers or collection of layers are dispersed.[8] There have been many studies conducted on rheological properties of polymer nanocomposites. Krishnamoorti and coworkers have worked on in situ polymerized nanocomposites with end-tethered polymer chains.[6,9] Hoffmann et al.[10] and Utracki and Lyngaae-Jørgensen[11] studied the rheological behavior of polyamide-12 and poly-ε-caprolactam nanocomposites, respectively. In these studies, it was reported that addition of layered silicates to polymers enhanced their linear viscoelastic properties (G', G''), and their power-law dependence at low frequencies were different from that of the unfilled polymers. Samples that were exfoliated displayed the greatest property enhancements compared with the intercalated ones. This was to be expected, as exfoliation would enable greater surface area of silicates to be exposed to the polymer chains.

Prasad et al.[12] have shown that ethylene-vinyl acetate (9 wt % EVA) nanocomposites exhibited pseudoplastic flow behavior at silicate concentration less than 5 wt %, with a clear Newtonian plateau followed by power-law dip in the steady shear viscosity profile. However, at higher silicate loadings, there was no Newtonian plateau in the low shear rate region, but a continuous shear thinning profile corresponding to the possible presence of finite yield stress.

In this study, we present the linear viscoelastic behavior of EVA copolymer nanocomposites using commercially modified clay. We investigated the effect of clay and vinyl acetate (VA) content on the linear viscoelastic response of these nanocomposites. The rheological characteristics will be used to demonstrate their relationship with the microstructure of these nanocomposites.

EXPERIMENTAL

Materials

EVA copolymers generally comprise ethylene backbone that has polar VA attached to it. The presence of the bulky polar pendent, VA, provides the ethylene backbone an opportunity to manipulate the end properties of the copolymer by varying and optimizing the VA content.[13]

The EVAs used in this project differed in their VA concentrations, giving rise to dissimilar properties. The VA concentrations in these EVAs were 18 and 28 wt %, respectively. In this text, these differing EVAs will be referred as EVA18 and EVA28, respectively. EVA18 and EVA28 were obtained from DuPont Packaging and Industrial Polymers (Australia). Table I gives the properties of these polymeric materials.

The organically modified montmorillonite (OMMT) clay used in this project was Cloisite® 30B (C30B) obtained from Southern Clay Products. C30B was a natural MMT (NA^+-MMT) modified with a ternary ammonium salt known as methyl, tallow, bis-2-hydroxyethyl quaternary ammonium (Fig. 1). This group of modified MMTs is suitable for the less hydrophobic polymers like EVA18 and EVA28. The cation exchange capacity of the clay was 90 meq/100 g, and it had a specific gravity of 1.98.

Preparation of EVA nanocomposites

The EVA pellets were initially premixed with the respective OMMTs before introducing into a Brabender twin-screw extruder. The extruder was operated at 100°C and at 70 rpm. EVA18 and EVA28 nanocomposites with clay loadings of 2.5, 5, and 7.5 wt % were produced. The extruded materials were then pelletized and compression molded at 120°C to yield samples of about 2 mm thickness.

Experimental techniques

Wide angle X-ray scattering

Wide angle X-ray scattering (WAXS) was used to analyze the extent of EVA intercalation into the silicate

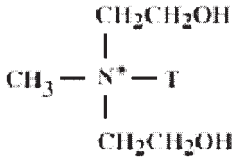

Figure 1 Ternary ammonium salt used in the production of C30B (where *T* is tallow (~65% C18; ~30% C16;~5% C14)). Anion, chloride.

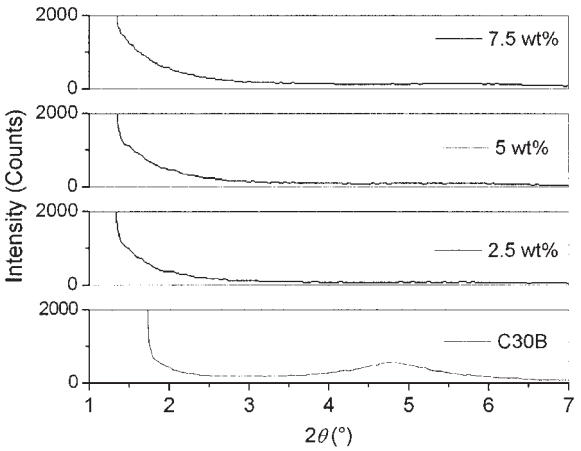

Figure 2 WAXS patterns comparing the *d*-spacing of C30B as well as EVA18–C30B nanocomposites, at loadings of 2.5, 5, and 7.5 wt %.

layers and hence the degree of layer swelling. WAXS data were obtained using Philips X-ray generator with 30 kV accelerating voltage and 30 mA current. Intensities from $2\theta = 1.2°$ to 30° were recorded using Ni filtered Cu-$K\alpha$ radiation ($\lambda = 0.154$ nm). XRD was conducted in transmission mode with 2-mm thick samples placed on a rotating sample holder and the sample was rotated during the scattering test. This type of sample holder can eliminate the effect of any possible orientation of the structure. Details of this method has been discussed elsewhere.[14] Background radiation has been removed from the scattering curves to be able to show scattering intensities up to 2θ of about 1.3°.

Transmission electron microscopy

WAXS techniques are very useful in determining basal spacing (or interlayer *d*-spacing) of ordered layered silicate structures. It may fall short when dealing with disordered intercalated or exfoliated structures, where no scattered intensity peaks will be observed and the lack of peaks may be construed as exfoliation.[15] For this reason, transmission electron microscopy (TEM) was found to be very useful, as it gave a pictorial view of what structure exists in the sample.

The TEM equipment used in this study was the JEOL 1010 with an accelerating voltage of 100 kV and high vacuum. The samples were ultramicrotomed using a diamond knife on a Leica Ultracut S with a liquid nitrogen-cooling (LNC) device. Operation of the LNC device at approximately −165°C was necessary as cutting EVA samples at room temperature was difficult because of the rubbery nature of these composites. The thickness of these cryogenically cut ultrathin sections was ~70 nm. These sections were then placed on copper grids, ready to be analyzed under TEM. The samples were magnified to 100,000×.

Small amplitude oscillatory shear

Small amplitude oscillatory shear measurements were conducted using the Advanced rheometrics expansion system (ARES) with parallel plate geometry. The tests were conducted using 25-mm diameter plates at 110°C. All measurements were performed with a force transducer with a range of 0.2–200*g* cm torque. A sinusoidally varying strain was applied and the resultant sinusoidal stress was measured. These dynamic frequency sweeps were useful in determining the microstructure and dynamics of the materials. The storage modulus, G', loss modulus, G'', and complex viscosity, η^*, estimates at very low frequencies were particularly relevant in comparing the linear viscoelastic characteristics of the EVA nanocomposites and the neat EVA copolymers.

These tests were conducted at low strain amplitudes that are within the linear viscoelastic region and at frequencies ranging from 100 rad/s to very low frequency of 0.001 rad/s. Determination of the linear viscoelastic region is essential before commencing tests for frequency sweep to ensure that the microstructure of the material would not be affected by shear alignment. The conditions that satisfy linear viscoelasticity are that the stress is linearly proportional to the imposed strain, and the torque response involves only the first harmonic.[16] In the linear viscoelastic region, both the storage and loss moduli are expected to be independent of strain amplitude, thus satisfying the first condition. The absence of higher harmonics for the stress response ensures that it remains sinusoidal, thus obeying the second condition.

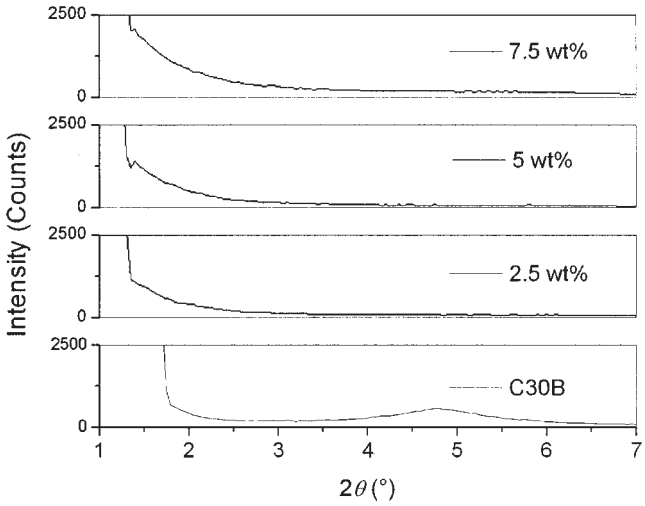

Figure 3 WAXS patterns comparing the *d*-spacing of C30B as well as EVA28–C30B nanocomposites, at loadings of 2.5, 5, and 7.5 wt %.

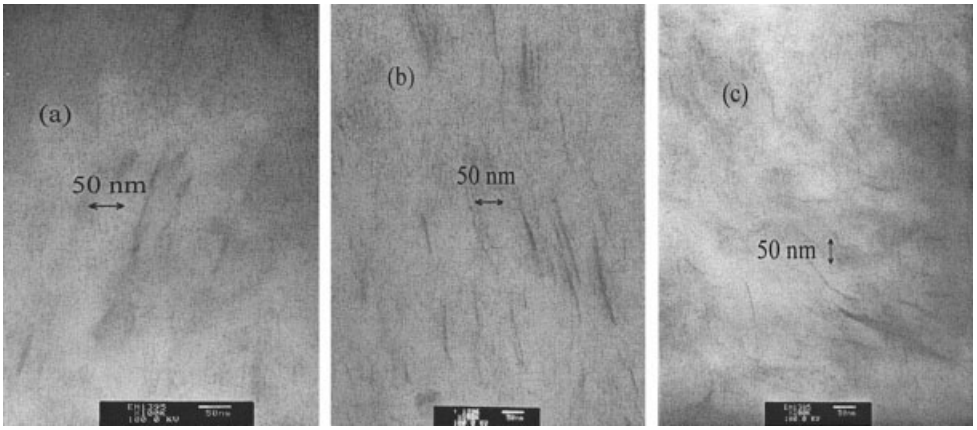

Figure 4 High magnification TEM images of EVA18 nanocomposites at C30B loadings of (a) 2.5 wt %, (b) 5 wt %, and (c) 7.5 wt %.

RESULTS AND DISCUSSION

Wide angle X-ray scattering

Figures 2 and 3 show WAXS curves for EVA18 and EVA28 nanocomposites. For comparison, scattering curves for C30B have been included. C30B has a high intensity, broad peak at $2\theta = 4.75°$. This gives a d_{001} spacing of 1.86 nm. This is in close agreement with that of the supplier[17] (1.85 nm) and similar studies conducted by Li and Ha[18] (1.88 nm). The results for EVA18 and EVA28 nanocomposites indicated that much of polymer chains had penetrated into the interlayer spaces of the layered silicates and expanded the basal distance. EVA18 nanocomposites, however, did not exhibit any discernible peaks at any of the scattering angles. This could be attributed to a high degree of dispersion of clay layers in the EVA18 matrix. Li and Ha[18] obtained similar results when they conducted WAXS studies on EVA18–C30B nanocomposites. But EVA28 nanocomposites did show low intensity shoulders at $2\theta = 1.4°$. This corresponds to d_{001} spacing of 6.3 nm. The presence of these shoulders may be due to any one of the reasons: (a) preferred thickness of the silicate layers, (b) it may have been a "cut-off" effect of the beam stop, hence not necessarily be a "real" peak as a result of layered silicate morphology. However, one can say that it is possible that the EVA28 nanocomposites possess either an exfoliated or disordered intercalated morphology similar to that of EVA18 nanocomposites.

Transmission electron microscopy

Figure 4(a–c) and Figure 5(a–c) illustrate TEM micrographs for EVA18 and EVA28 nanocomposites, respectively. The higher electron density of the silicates relative to the EVA matrix gives them a much darker appearance. The absence of Bragg peaks in WAXS (Fig. 2) suggests that EVA18 nanocomposites exhibit exfoliated or disordered intercalated morphologies. However, the TEM images showed otherwise. All the EVA18 nanocomposites exhibited mixed intercalated/

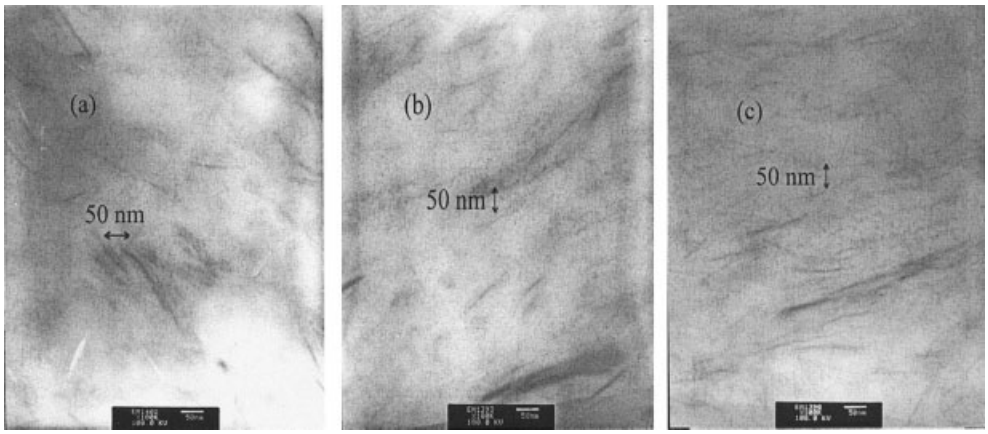

Figure 5 High magnification TEM images of EVA28 nanocomposites at C30B loadings of (a) 2.5 wt %, (b) 5 wt %, and (c) 7.5 wt %.

exfoliated morphologies. The presence of stacks of silicate layers shows the presence of intercalation, while individual layers suggest exfoliation. The images also reveal that the melt mixing process had not only segregated the silicate agglomerates, but also distributed them quite well in the EVA18 matrix.

The TEM images for EVA28 nanocomposites reveal similar results as that obtained for EVA18 nanocomposites in that they too exhibit mixed intercalated/exfoliated morphologies. From these images, exfoliated individual layers could be seen interspersed with silicate stacks that are a few layers thick. Moreover, the melt mixing process had indeed distributed the silicate layers very well in the EVA28 matrix. Both sets of TEM images also show that increasing the concentration of silicates from 2.5 to 7.5 wt % increases the surface area of contact of silicates with the polymer matrix. This increase in packing density of silicates with concentration has a direct impact on their linear viscoelastic properties. This effect will be discussed in the next section. Observation of WAXS and TEM results gives the impression that C30B is in fact a suitable filler for EVA18 and EVA28, although complete exfoliation of layered silicates had not been achieved. Li and Ha[18] and Duquesna et al.[19] obtained similar morphology with their EVA nanocomposites. However, Duquesna et al.[19] used EVA with 19 wt % VA–C30B systems. Alexandre et al.[20] studied EVA with 27 wt % VA nanocomposites with layered silicates modified using dimethyl-dioctadecyl quaternary ammonium and dimethyl-2-ethylhexyl quaternary ammonium. They too observed mixed morphologies irrespective of silicate modifiers used, although the extent of exfoliation was much higher with the use of the former modifier.

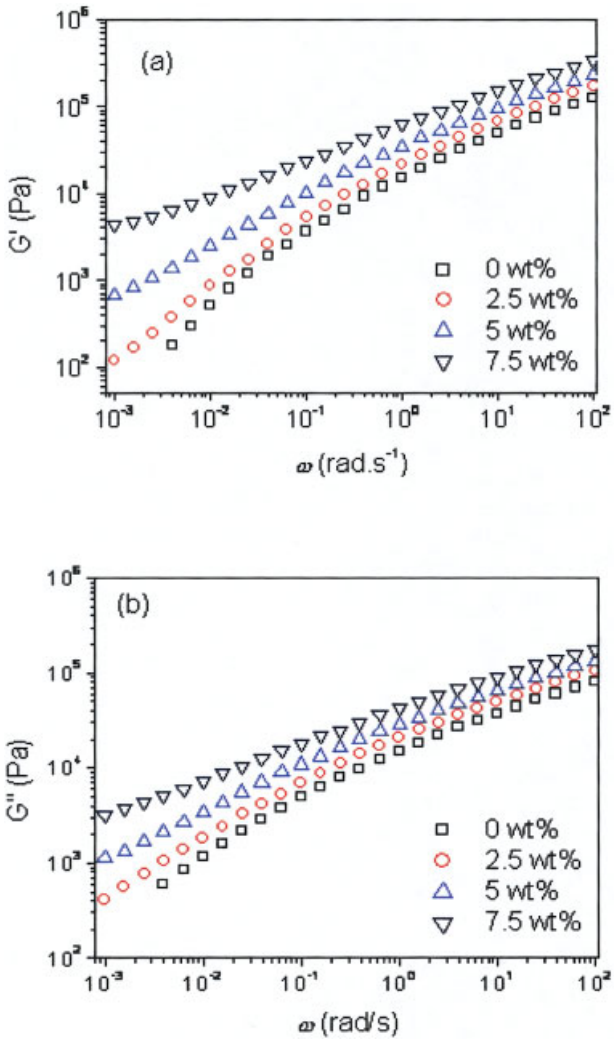

Figure 6 Dynamic frequency sweep results for EVA18 nanocomposites (a) storage moduli (G') and (b) loss moduli (G''), at 110°C. [Color figure can be viewed in the online issue, which is available at www.interscience.wiley.com.]

Small amplitude oscillatory shear

The effects of fillers on rheological properties of polymer–filler conventional composites and nanocomposites have been studied extensively.[1–4,6,8–11] The general consensus is that polymer–filler and filler–filler interactions strongly affect the rheological behavior (hence processing) of these composites.

The oscillatory behaviors of EVA18 and EVA28 nanocomposites are shown in Figure 6(a, b) and Figure 7(a, b), respectively. Clearly, both sets of nanocomposites exhibit an increase in G' and G'' at all frequencies. The enhancement of both moduli is especially so in the low frequency region compared with the high frequency region. As stated earlier in this article, increase in silicate concentration increases the solid-like or elastic nature of the nanocomposites. The strong viscoelastic improvements demonstrated by these nanocomposite systems is considered to be remarkable. This is so because in conventional composites (or microcomposites), it would take much higher concentrations of fillers to give these improvements.[2,21–23] Similarly, G'' too showed improvements. G'' is a viscoelastic parameter that indicates the viscous or liquid-like nature of the material, and it gives information on the viscous or energy dissipation during flow.[24] The layered silicates, at low frequencies, increase the G'', but at higher frequencies these anisotropic silicate platelets or stacks of platelets get aligned in the direction of flow. Because of this alignment, the effective contribution to moduli enhancement is less. The limited contribution at the high frequency region is observed for the storage and loss moduli of both sets of nanocomposites.

An important feature that is raised when discussing storage and loss moduli of materials is their slope at low frequencies. This slope characterizes the quiescent nature of these nanocomposites. Ferry[16] noted that for noncrosslinked homopolymers, the power-law linear viscoelastic slopes can be expressed as $G' \propto \omega^2$ and $G'' \propto w^1$ (and $\eta^* \propto w^0$). This is typical for homopolymers

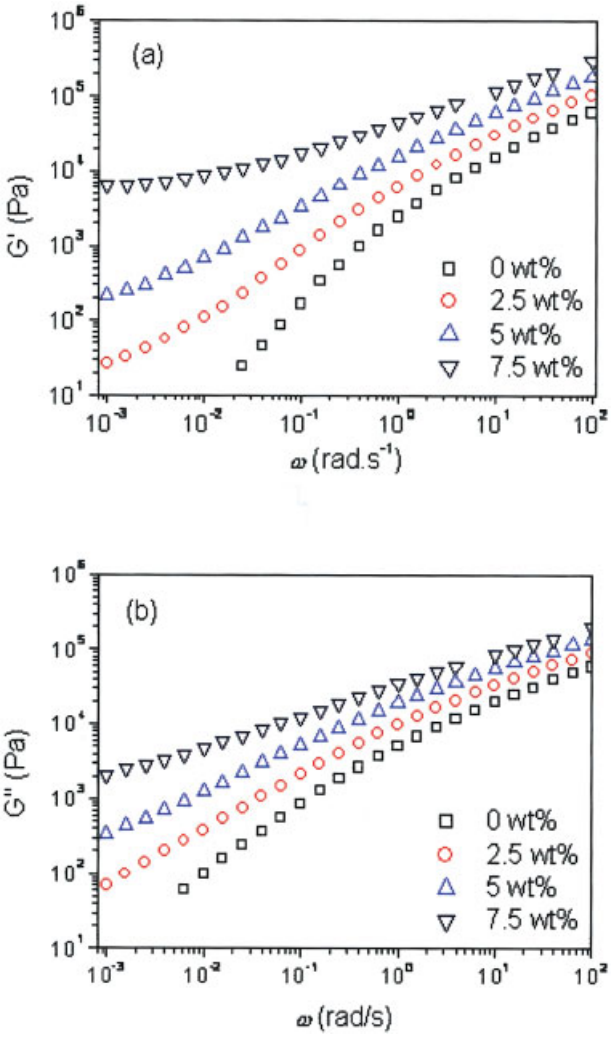

Figure 7 Dynamic frequency sweep results for EVA28 nanocomposites (a) storage moduli (G') and (b) loss moduli (G''), at 110°C. [Color figure can be viewed in the online issue, which is available at www.interscience.wiley.com.]

that behave as Newtonian fluid and exhibit terminal behavior at low frequencies. For nanocomposites, the slopes of moduli at low frequencies could be used to analyze their quiescent structure.

Figure 8 shows the slope of G' versus ω curve at low frequencies. G' has been used here because it is the most sensitive rheological function to changes in the mesoscopic structure of the nanocomposites. This slope has been labeled as α. It is quite clear from Figure 8 that increasing the silicate content decreases the slope, α. Independence of G' ($\alpha \sim 0$) with respect to ω would mean pseudosolid-like characteristic. The slope, α, as shown in Figure 8 decreases with silicate loading, with a discontinuity at 2.5 wt % for both EVA18 and EVA28 nanocomposites. The discontinuity marks the percolation threshold of EVA18 and EVA28 nanocomposites. This threshold corresponds to the formation of three-dimensional network structure, whereby silicate layers act as physical crosslinkers, hence a mesostructure with enhanced silicate–silicate interactions.

Percolation is the process of network formation by random filling of bonds (or sites) on a lattice, or by random filling of regions in space.[25] De Gennes[26] explained that percolation theory was developed from a statistical model that was used to establish how a given set of sites (regularly or randomly distributed in space) is interconnected according to a defined bonding criterion. Surpassing the percolation threshold, a topological singularity occurs. This singularity signifies connections between sites on a larger scale. At low filler fractions, the particles are percolated within the matrix. When the filler fraction has reached its maximum packing fraction (corresponding to percolation threshold),[27] the polymer is entrapped within the interstices of the filler network. This observation has been made earlier from the TEM images, which showed that increasing silicate loading increases the packing density of silicates in the matrix. This is particularly so when much of the original clay tactoids or agglomerates had been well dispersed and distributed within the matrix, thereby increasing the surface area of contact between the polymer matrix and silicate layers.

The frequency dependence of the filled nanocomposite system reported here is similar to many other polymer nanocomposite systems, with intercalated or exfoliated morphologies.[6,8,28,29] Mitchell and Krishnamoorti[30] have also demonstrated that even for exfoliated (or disordered intercalated) laponite-based nanocomposites, no percolation limit was observed, consistent with the absence of a network structure.

It is interesting to note that the change in slope (α) with respect to silicate content is more drastic for EVA28 compared with EVA18, although both nanocomposites were found to have mixed intercalated/exfoliated morphologies. This could be due to the higher degree of interactions between the carboxyl groups of the EVA28 chains and hydroxyl groups of the ammonium cations on the surface of the silicate layers compared with that of EVA18.[18] It must be noted here that EVA28 is the more polar of the two EVA polymers.[31] Moreover, it must be noted that unlike the filled systems, the neat copolymers were

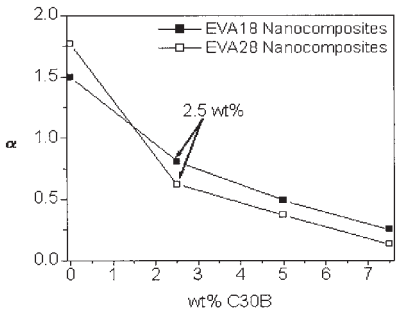

Figure 8 α (slope of G' at low frequency) as a function of silicate loading (wt %) EVA18 and EVA28 nanocomposites, at 110°C.

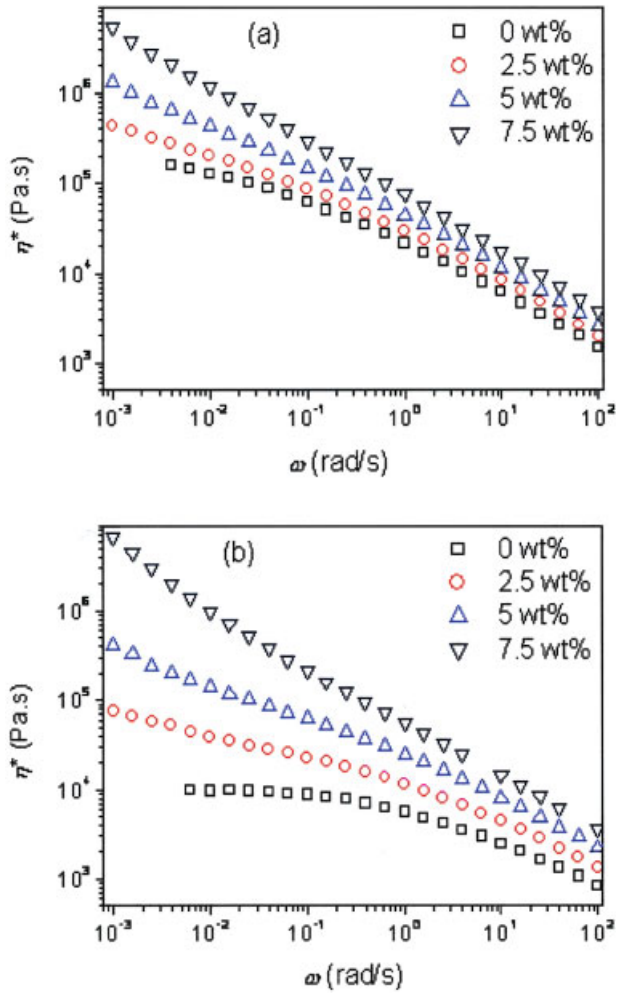

Figure 9 Complex viscosity profile of (a) EVA18 and (b) EVA28 nanocomposites, at 110°C. [Color figure can be viewed in the online issue, which is available at www.interscience.wiley.com.]

not subjected to low frequency ranges in the vicinity of 0.001 rad/s. A consequence of this will be discussed later in this article.

Figure 9(a, b) shows the complex viscosity (η^*) profiles of EVA18 and EVA28 nanocomposites. Akin to the storage and loss moduli representations shown in Figures 6 and 7, the complex viscosities also showed differences in filled EVA behavior compared with that of the unfilled system. Evidently, as the filler concentration was increased, the complex viscosity increased at all frequencies tested. At high frequencies, there was a clear shear-thinning characteristic due to the alignment of the anisotropic fillers in the direction of shear. At low frequencies, the nanocomposites exhibited a divergence in viscosities, as silicate loading was increased. The divergence was similar to that of storage moduli as shown earlier (Figs. 6 and 7), where at low frequencies the G' diverged from a terminal slope (Newtonian) to that of a near solid-like constant moduli (equilibrium moduli) behavior irrespective of frequency.

Similar to the equilibrium modulus signifying elastic nature of a material, the divergence of complex viscosity profile at low frequencies suggest the possibility of a finite yield stress. The presence of yield stress is related to the concentration and strength of a material formed as a result of polymer–filler and filler–filler interactions. Doremus and Piau[32] explained that materials with yield stress are formed from at least two components. The compounding of polymers with fillers results in addition to polymer–polymer entanglements and polymer–filler junctions. They proposed that the presence of these junctions due to the absorption of polymer chains is in fact the basis of yield stress. Besides filled polymeric melts and suspensions, non-Newtonian divergence and the formation of equilibrium moduli have also been reported for block copolymers with ordered microdomains (spherical, lamellar, or cylindrical).[25] The mechanisms for yield in these materials have been attributed to the presence of undulations and/or topological defects in the layers.[33,34]

Rheologically, the presence of yield stress is characterized with a shear (steady or oscillatory) viscosity slope of −1 in the low frequency domain. The transition from Newtonian plateau to non-Newtonian divergence of complex viscosity at low frequencies could be analyzed from the power-law slopes, as shown in Table II.

For both sets of nanocomposites, the slopes increased, even though negatively (corresponding to divergence). The highest slope values attained were for 7.5 wt % EVA18 and EVA28 systems. Both these did not produce slopes of −1, which would confirm the presence of a finite yield stress. The presence of yield stress indicates a network structure, as mentioned earlier. The complex viscosity results are similar to that of storage modulus response, which did not quite achieve a plateau (relating to equilibrium moduli) in the low frequency region. However, the nonattainment of finite yield stress does not preclude the presence of three-dimensional network structure. It only signifies that the network structure is not as prevalent as in a pure elastic material.

TABLE II
Power-law Slopes of Complex Viscosity Versus Frequency Curves in the Low Frequency Region for EVA18 and EVA28 Nanocomposites at 110°C

EVA18 nanocomposites (wt %)	Slope (low ω)	EVA28 nanocomposites (wt %)	Slope (low ω)
0	−0.25	0	~0
2.5	−0.33	2.5	−0.28
5	−0.49	5	−0.46
7.5	−0.67	7.5	−0.84

It must be noted that the percolated network or three-dimensional network systems formed in polymer nanocomposites are different to some extent to networks found in other polymeric systems. It is perhaps relevant at this juncture to provide a brief comparison between the network structure in polymeric nanocomposites and that of other polymeric systems.

In linear homopolymers for instance, network formation is a result of interactions due to physical interlocking of chains (chain entanglements) and are considered temporary. Graessley[35] explained that chain entanglements could be viewed as a type of intermolecular interactions that affects large-scale motions of chains and thus the long time end of the viscoelastic relaxation spectrum. In the terminal region, the storage moduli of these entangled systems fall drastically from the glassy moduli (high frequency region). This signifies time scales that are long enough to allow for the disentanglements of the networks, resulting in relaxation.[36] Increasing the molecular weight or degree of branching of the polymer chains only serve to shift the complete relaxation to longer time scales (corresponding to lower frequencies).[16] This is so because in polymers with a higher degree of entanglements, the formation of knots slows down their ability to relax their interactions with neighboring chains, and the presence of branch points retards motion along their backbone.[36]

Besides physical interlocking of chains, chain architecture with chemical interlocking or crosslinking produces a form of stronger structure as seen in polymeric gels. This sort of crosslinking is via chemical reaction (although physical crosslinking due to intermolecular forces and chain entanglements are also present). According to the percolation theory,[25,37] the chemical reaction relates to the conversion of unfilled bonds to filled bonds and as the fraction of filled bonds are increased, clusters of bonds are formed, and eventually percolation transition is reached. This critical point is marked by infinite, lattice-wide cluster formation. Ferry[16] explained that the introduction of crosslinks into an uncross-linked system converts its behavior from a viscoelastic liquid to a viscoelastic solid. Goodwin and Hughes[38] wrote that with increased crosslink formation, polymer gels are able to store energy. The material experiences an increase in storage modulus and a reduced capacity to dissipate viscous energy. The network formed experiences an inability to completely relax, resulting in an equilibrium modulus in the low frequency region (long time scale).

In the case of EVA nanocomposites, it is quite obvious from linear viscoelastic measurements (Figs. 6, 7, and 9) that EVA28 nanocomposites displayed a more pronounced elastic characteristic compared with EVA18 nanocomposites. This was attributed to the higher degree of interactions between the carboxyl groups of the EVA28 chains and the hydroxyl groups of the ammonium cations on the surface of the silicate layers compared with that of EVA18. The concentration of polar VA groups in EVA28 is much higher than that of EVA18, thereby producing greater amount of tethering of EVA28 onto the layered silicates. The higher extent of EVA adsorption onto silicate surfaces is analogous to the formation of crosslinks in polymer gels and vulcanized rubbers. The tethering of chains onto the silicate surfaces restricts the relaxation process and according to Witten et al.[39] this is due to the creation of an energetic barrier that reduces reptation motion. The reduction in reptation motion results in an increase in relaxation times, at very low frequencies (shift in terminal zone to longer time scales). However, during the relaxation process proceeding from high frequencies to low frequencies, the reformation of an extensive network structure may in fact store energy within the network rather than dissipate it. This is manifested in the presence of a pseudoequilibrium plateau at long time scales, especially for the 7.5 wt % nanocomposites. Table III shows the characteristic relaxation times (ω_c^{-1}) as obtained from crossover point of G' and G''.[25]

TABLE III
Characteristic Relaxation Times for EVA18 and EVA28 Nanocomposites at 110°C Obtained from the Crossover Point of G' and G''

EVA18 nanocomposites (wt %)	Characteristic relaxation time (s)	EVA28 nanocomposites (wt %)	Characteristic relaxation time (s)
0	1	0	0.016
2.5	1.59	2.5	0.04
5	6.67	5	0.25
7.5	—	7.5	—

The relaxation time is the inverse of the crossover frequency (ω_c^{-1}). No crossover was detected for both EVA with 7.5 wt % C30B, indicative of a pseudosolid-like structure, with extensive network capable of storing energy.

A final point of discussion is the linear viscoelastic behavior of unfilled EVA18 and EVA28. Figure 10 shows the G' and η^* response of both EVA copolymers under oscillatory shear. It must be noted that unlike the filled systems, both neat EVA copolymers were not subjected to tests in the low frequency vicinity of 0.001 rad/s. Quite clearly, EVA18 showed much higher viscoelastic responses compared with EVA28 at all frequencies, at a test temperature of 110°C. EVA28 chains could be said to have achieved complete relaxation (or near complete) in short time scales (Table III), and this is characterized by a power-law slope of 1.77 for the storage modulus in the terminal region and a clear Newtonian plateau. EVA18 chains, on the other hand, had not exhibited clear Newtonian plateau (slope of -0.25) or a power-law slope for G' close to that of EVA28. This is clearly shown in Figure 10. This response for EVA18 showed that its chains had not reached complete relaxation and slightly

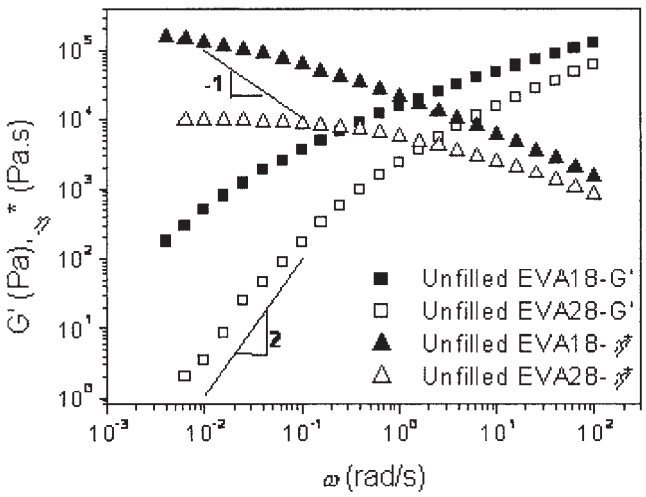

Figure 10 Comparing linear viscoelastic response of unfilled EVA18 and EVA28 polymers.

longer time scales would be required, relating to a shift to lower frequencies. A reason for the difference in responses from both EVAs is the presence of the polar VA group. EVA copolymers with low VA content are essentially a modified version of low density polyethylenes (LDPE).[40] This simply means that compared with EVA28, EVA18 has a high degree of branching[41] that amounts to the formation of chain entanglements, and as mentioned earlier, the presence of chain entanglements would shift relaxation times to lower frequencies as evident from the relaxation times for EVA18 and EVA28, as given in Table III.

CONCLUSIONS

Polymer nanocomposites were prepared by melt blending EVA18 and EVA28 with Cloisite® 30B. The nanocomposites produced were analyzed using WAXS and TEM, and were deemed to have mixed intercalated/exfoliated morphologies. Oscillatory shear measurements revealed enhanced linear viscoelastic response with loading at all frequencies tested. The gradual disappearance of terminal behavior and Newtonian liquid-like behavior was observed, relating to the formation of a three-dimensional network structure that has the capacity to store elastic energy. Linear viscoelastic behavior revealed differences between neat EVA18 and EVA28, possibly due to the extent of branching entanglements.

References

1. Milewski, J. W.; Katz, H. S. In Handbook for Fillers and Reinforcements for Plastics; Milewski, J. W.; Katz, H. S., Eds.; Van Nostrand Reinhold: New York, 1978; Chapter 1, p 3.
2. Shenoy, A. V. Rheology of Filled Polymer Systems; Kluwer Academic: Dordrecht, 1999.
3. Tanaka, H.; White, J. L. Polym Eng Sci 1980, 20, 949.
4. Laun, H. M. Colloid Polym Sci 1984, 262, 257.
5. Giannelis, E. P. Appl Organometal Chem 2001, 12, 675.
6. Giannelis, E. P.; Krishnamoorti, R.; Manias, E. Adv Polym Sci 1999, 138, 107.
7. LeBaron, P. C.; Wang, Z.; Pinnavaia, T. J Appl Clay Sci 1999, 15, 11.
8. Krishnamoorti, R.; Silva, A. S. In Polymer–Clay Nanocomposites; Pinnavaia, T. J.; Beall, G. W., Eds.; Wiley: New York, 2000; p 315.
9. Krishnamoorti, R.; Giannelis, E. P. Macromolecules 1997, 30, 4097.
10. Hoffmann, B.; Kressler, J.; Stöppelmann, G.; Friedrich, Chr.; Kim, G. M. Colloid Polym Sci 2000, 278, 629.
11. Utracki, L. A.; Lyngaae-Jørgensen, J. Rheol Acta 2002, 41, 394.
12. Prasad, R.; Pasanovic-Zujo, V.; Gupta, R. K.; Cser, F.; Bhattacharya, S. N. Polym Eng Sci 2004, 44, 1220.
13. Baker, A.-M. M.; Mead, J. In Thermoplastics in Modern Plastics Handbook; Harper, C. A., Ed.; McGraw-Hill: New York, 2000.
14. Cser, F.; Bhattacharya, S. N. J Appl Polym Sci 2003, 90, 3026.
15. Morgan, A. B.; Gilman, J. W. J Appl Polym Sci 2003, 87, 1329.
16. Ferry, J. D. Viscoelastic Properties of Polymers, 3rd ed.; Wiley: New York, 1980.
17. Southern Clay Products (SCP). Cloisite Data Sheets; www.scprod.com (accessed 10 June 2004).
18. Li, X.; Ha, C.-S. J Appl Polym Sci 2003, 87, 1901.
19. Duquesna, S.; Jama, C.; Le Bras, M.; Delobel, R.; Recourt, P.; Gloaguen, J. M. Compos Sci Technol 2003, 63, 1141.
20. Alexandre, M.; Beyer, G.; Henrist, C.; Cloots, R.; Rulmont, A.; Jérôme, R.; Dubois, P. Macromol Rapid Commun 2001, 22, 643.
21. Khan, S. A.; Prud'homme, R. K. Rev Chem Eng 1987, 4, 205.
22. Hornsby, P. R. Adv Polym Sci 1999, 139, 156.
23. Wu, G.; Asai, S.; Sumita, M.; Hattori, T.; Higuchi, R.; Washiyama, J. Colloid Polym Sci 2000, 278, 220.
24. Greene, J. P.; Wilkes, J. O. Polym Eng Sci 1995, 35, 1670.
25. Larson, R. G. The Structure and Rheology of Complex Fluids; Oxford University Press: New York, 1999.
26. De Gennes, P .G. Scaling Concepts in Polymer Physics; Cornell University Press: New York, 1979.
27. Mele, P.; Alberola, N. D. Compos Sci Technol 1996, 56, 849.
28. Lim, Y. T.; Park, O. O. Rheol Acta 2001, 40, 220.
29. Solomon, M. J.; Almusallam, A. S.; Seefeldt, K. F.; Somwangthanaroj, A.; Varadan, P. Macromolecules 2001, 34, 1864.
30. Mitchell, C. A.; Krishnamoorti, R. J Polym Sci Part B: Polym Phys 2002, 40, 1434.
31. Tang, L. W.; Tam, K. C.; Yue, C. Y.; Hu, X.; Lam, Y. C.; Li, L. Polym Int 2002, 51, 325.
32. Doremus, P.; Piau, J. M. J Non-Newtonian Fluid Mech 1991, 39, 335.
33. Koppi, K. A.; Tirrell, M.; Bates, F. S.; Almdal, K.; Colby, R. H. J Phys II 1992, 2, 1941.
34. Larson, R. G.; Winey, K. I.; Patel, S. S.; Watanabe, H.; Bruinsma, R. Rheol Acta 1993, 32, 245.
35. Graessley, W. W. Adv Polym Sci 1974, 16, 1.
36. Morrison, F. A. Understanding Rheology; Oxford University Press: New York, 2001.
37. Isichenko, M. B. Rev Mod Phys 1992, 64, 961.
38. Goodwin, J. W.; Hughes, R. W. Rheology for Chemists: An Introduction; Royal Society of Chemistry: Cambridge, 2000.
39. Witten, T. A.; Leibler, L.; Pincus, P. Macromolecules 1990, 23, 824.
40. Brydson, J. A. Plastics Materials; Newnes-Butterworths: London, 1975.
41. Arsac, A.; Carrot, C.; Guillet, J. J Appl Polym Sci 1999, 74, 2625.